Proceedings of The National Conference
On Undergraduate Research (NCUR) 2013
University of Wisconsin La Crosse, WI
April 11 – 13, 2013

High-Frequency Ultrasound of Breast Tissue Phantoms Containing Microscopic Heterogeneities

Joseph E. Roring
Department of Physics
Utah Valley University
800 West University Parkway
Orem, Utah 84058 USA

Faculty Advisor: Dr. Timothy E. Doyle

Abstract

Removal of all cancerous tissue in breast conservation surgery (BCS) is critical to prevent local recurrence. Unfortunately, 30-50% of patients require additional surgery due to failure to resect all the necessary tissue. A real-time method for detecting infected tissue is therefore desirable. Previous studies have shown that the complexity of high-frequency (50 MHz) ultrasonic spectra can be correlated to a range of breast pathologies in BCS. However, the mechanism behind this correlation is still not very well understood. The purpose of this research is to explore the connection between tissue micro-heterogeneity and ultrasonic spectral complexity using breast tissue phantoms, i.e. materials that mimic breast tissue properties and microstructure. A physical basis can then be determined that links ultrasonic measurements to breast tissue pathology. Phantoms were made from a Knox® gelatin base and soluble fiber (Metamucil®). Heterogeneities simulating lobular and ductal components of mammary glands were created through the addition of polyethylene microspheres and nylon fibers. Pitch-catch and pulse-echo waveforms were acquired from the samples using high-frequency ultrasound. The data were analyzed by measuring the number of peaks (the peak density) in the first-order spectrum (Fourier transform of the time-domain waveform) and the slope of the second-order spectrum (two consecutive Fourier transforms of the time-domain waveform). The phantom specimens displayed first-order peak densities that were significantly greater and second-order spectral slopes that were significantly lower than homogeneous control samples. Phantoms with large fibers (250 micrometer diameter) showed the highest peak densities with values greater than 3x those of the controls. The peak density trend of the phantom samples with increased microscopic heterogeneity was consistent with data of breast tissue specimens. These results provide a physical mechanism for the use of these parameters in the imaging of breast tissues with atypical and malignant pathologies.

Keywords: High-Frequency Ultrasound, Breast Cancer Detection, Real Time Pathology

1. Introduction

Obtaining negative (cancer free) margins in breast conservation surgery (BCS) is critical for local control of cancer in the affected breast and reducing re-excision rates.[1-5] A study of 994 women with ductal carcinoma *in situ* (DCIS) showed that long-term ipsilateral disease-free survival strongly correlated with margin status, and that positive or close margins following the last surgical treatment significantly reduced 5-year and 10-year ipsilateral event-free survival independent of treatment strategy.[6] Negative margins are particularly difficult to achieve for invasive lobular carcinoma (ILC), with six studies reporting 49-63% positive or close margins following the initial surgery, and one study reporting 39% positive or close margins with the use of full thickness excision and oncoplastic surgery.[7]

Touch preparation cytology and frozen section analyses are currently being used for the intraoperative histopathology of margins, but are limited by the inability to identify close margins (touch preparation cytology), the ability to sample only a small portion of the margin (frozen section analyses), and the need for an on-site trained pathologist.[8-12] Other methods are therefore being investigated to estimate margin sizes both before and during surgery, including pre-operative CT and MRI,[13] high-resolution two-dimensional specimen mammography,[14] Raman spectroscopy,[15,16] optical coherence tomography,[17] diffuse reflectance spectroscopy,[12,18] terahertz wave imaging,[19] and radiofrequency spectroscopy.[20,21]

Ultrasound has also been researched for the intraoperative assessment of margins with standard clinical instrumentation, imaging modalities, and frequency ranges (7.5-14 MHz).[3,22-26] Results show a significant reduction in positive margin resection rates from 41% to 9%,[24] 17.5% to 3.6%,[26] and 29% to 3.5%.[3] Since the approach relies on the detection of tumor edges from the interpretation of sonograms, an experienced radiologist is required during the surgery.

A pilot study by Doyle *et al.* recently showed that high-frequency (HF) ultrasound (20-80 MHz) may be able to differentiate between normal, benign, and malignant pathologies in resected margin specimens based on the spectral signatures in the ultrasonic signals.[27] The method differed from standard clinical ultrasound in that excised margins were examined by placing the margins between opposing transducers. Measurements were taken using both a through-transmission mode where one transducer is a transmitter and the other is a receiver, and a pulse-echo mode where the pulse travels through the margin, reflects from the hard wear-face of the opposing transducer, and travels back to the transmitting transducer.

Doyle *et al.* also used signal processing techniques that differed from standard clinical ultrasound.[27] The structure of both the first-order spectra, corresponding to one Fourier transform of the time-domain waveform, and the second-order spectra, corresponding to two successive Fourier transforms of the time-domain waveform, were analyzed and correlated to margin pathology. The results showed that two parameters were independently sensitive to margin pathology and could be used to differentiate between normal, benign, and malignant breast pathologies. These parameters were the number of peaks and valleys, heretofore called the peak density, in the first-order spectra, and the slope of the log-normal second-order spectra.

Since the first-order peak density (henceforth referred to as peak density) and second-order spectral gradient (henceforth referred to as spectral gradient) were sensitive to the pathology of breast tissue, it is hypothesized that changes in these parameters can be attributed to modifications in the tissue microstructure that give rise to changes in the ultrasonic scattering properties of the tissue. The primary modification in tissue microstructure is the degree of heterogeneity present, which increases ultrasonic scattering by increasing the number of scattering sites or surfaces. An increase in scattering leads to an increase in spectral structure due to multiple scattering, interference effects between tissue structures, or preferential enhancement or suppression of forward scattering at specific frequencies due to changes in the geometry and size of scatterers.

To test this hypothesis, gelatin-based phantoms were made with polyethylene microspheres and nylon fibers to simulate breast tissue with a range of heterogeneous microstructures. The solid microspheres and fibers were chosen to simulate lobular and ductal architectures with hyperplastic or malignant pathologies. The phantoms were tested with HF ultrasound following procedures developed for resected margins.[27]

2. Methods

Phantom specimens with tissue-like ultrasonic properties were made using a formula comprised of gelatin (Knox® gelatin) and psyllium fiber (Metamucil®).[28] Polyethylene microspheres with diameters ranging from 58-390 μm and nylon fibers of 10-mm length and diameters ranging from 130-250 μm were mixed into the phantoms prior to gelling. Table 1 shows the sample matrix and final volume concentrations of inclusions after mixing. Three control samples were also made with no inclusions. Phantoms were cast into disk-shaped samples of 45-mm diameter and 20-mm thickness.

The introduction of solid microsphere and fiber inclusions into phantoms resulted in microstructures that approximated several common breast pathologies. The homogeneity of control samples corresponded to the stromal proliferation and loss of ductal architecture as found in fibroadenomas. The cylindrical geometry of the solid fibers corresponded to the proliferation of cells within breast gland ducts as found in atypical ductal hyperplasia or DCIS. The small microspheres corresponded to the proliferation of cells within lobules as found in LCIS. Finally, the large microspheres corresponded to small, sub-millimeter tumors as found in invasive ductal carcinoma (IDC).

Table 1. Phantom sample matrix.

Inclusion	Diameter (μm)	Volume Concentration (%)		
Polyethylene Microspheres	58 ± 5	2.5	5.0	10.
	98 ± 8	2.5	5.0	10.
	196 ± 16	2.5	5.0	10.
	390 ± 35	2.5	5.0	10.
Nylon Fibers	130	1.4		
	180	4.9		
	240	7.1		
	250	6.5		

Through-transmission and pulse-echo data were acquired from phantom specimens with the use of the experimental setup shown in Figure 1. An aluminum test fixture (left, Figure 1) was used to support the specimen and to position the two ultrasonic immersion transducers (Olympus NDT, V358-SU, 50 MHz, 0.635-cm dia. element) above and below the sample for measurements. A HF square-wave pulser-receiver (UTEX, UT340, middle bottom, Figure 1) and a digital storage oscilloscope (Hewlett-Packard, HP-54522A, 500 MHz, 1Gs/s, middle top, Figure 1) were used to generate the ultrasonic pulses, amplify the received signals, and digitize the waveforms. Waveforms were averaged during signal acquisition and downloaded onto a notebook PC using LabVIEW (right, Figure 1). The specimen thickness was recorded for each ultrasonic measurement.

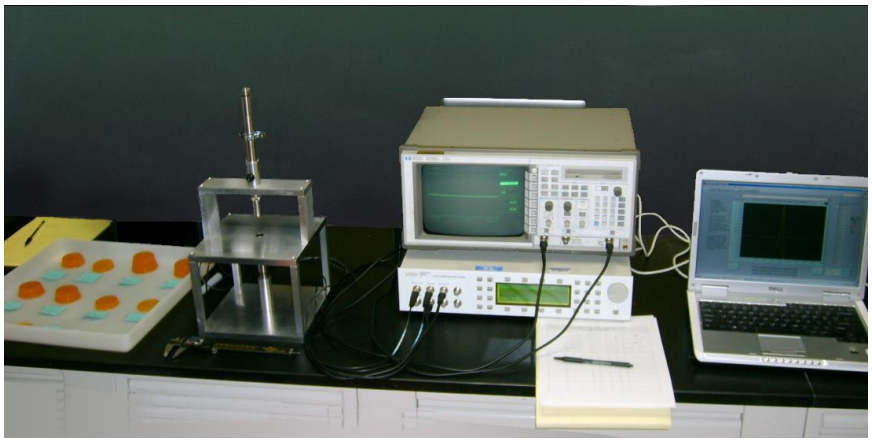

Figure 1. Photograph of experimental setup for acquiring HF ultrasonic data from phantom specimens with introduced heterogeneities, including (from left to right) phantom specimens, aluminum test fixture, digital oscilloscope (top) with ultrasonic pulser-receiver (bottom), and notebook PC.

The ultrasonic measurements produced signals that were substantially different from ultrasonic signals typically acquired for medical imaging or tissue characterization. Ultrasound signals used for medical imaging arise from dispersed scattering centers, typically cells, nuclei, and tissue inhomogeneities such as blood vessel walls. The resulting signals are therefore from diffuse reflection. In contrast, the signals collected in this study were of the transmitted pulse after propagating through the tissue specimen, either in through-transmission mode or pulse-echo mode where the pulse experiences specular reflection from the surface of the second transducer. The signals were therefore pulse-like with amplitudes significantly greater than background noise.

The ultrasonic data were analyzed in the frequency (spectral) domain since previous experimental and numerical studies had indicated that the structure of HF ultrasonic spectra were sensitive to neoplastic changes in breast tissues.[27,29-31] The spectral signatures were additionally robust and insensitive to sample variations such as thickness and attenuation.[27]

First-order power spectra were obtained by subtracting background waveforms from the phantom waveforms, windowing the main signals in the waveforms, padding the waveforms to 4000 points to increase the spectral resolution, performing a fast Fourier transform (FFT), and then taking the absolute value of the complex spectra.

The peak density was calculated by counting the number of zero crossings of the derivative of the spectrum in the 20-80 MHz band. Figure 2(a) displays examples of ultrasonic spectra from fibroadenoma, normal, and LCIS tissue specimens obtained during BCS, showing progressively increasing peak densities with microstructural heterogeneity.[27] Figure 2(b) displays examples of ultrasonic spectra from corresponding phantom microstructures, again showing progressively increasing peak densities with microstructural heterogeneity.

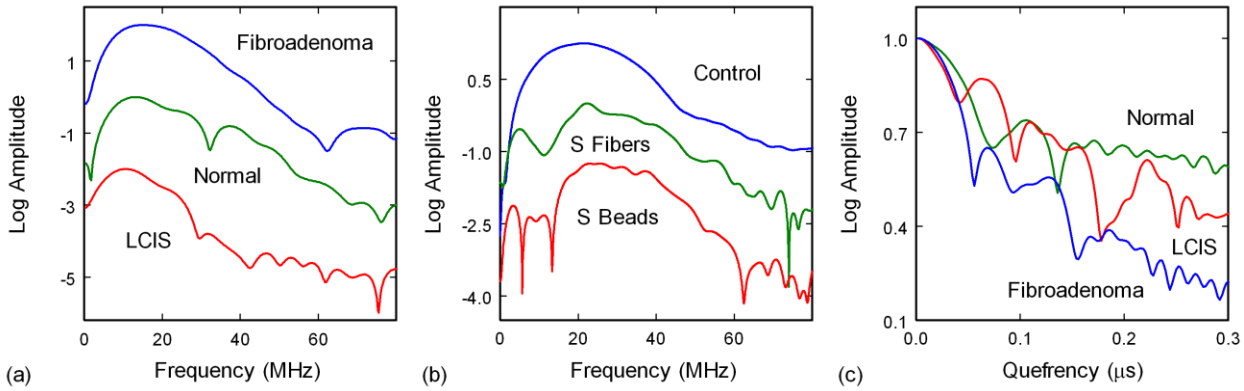

Figure 2. (a) HF through-transmission ultrasonic spectra of margins and other breast tissue specimens from breast conservation surgery. (b) HF through-transmission ultrasonic spectra of phantoms with small fibers (130-180 μm diameter) and small beads (196-μm diameter). (c) HF pulse-echo second-order spectra of margins and other breast tissue specimens from breast conservation surgery. Spectra are offset in (a) and (b) for clarity.

Second order power spectra of the waveforms were obtained by performing a second forward FFT on the first-order spectra, taking the absolute value of the complex function, and normalizing the curves. The second-order spectra showed a maximum at 0 μs and sloped downward with multiple peaks at various positions. The spectral gradient was determined by calculating the slope of the log of the second-order spectrum, which was approximately linear in the 0-0.3 μs range. Figure 2(c) shows second-order power spectra of margins and other breast tissue specimens from BCS.[27] The peak density and spectral gradient data were evaluated using the median and median absolute deviation (MAD) to compare the phantom microstructures both within the sample set and with breast tissue results.

3. Results and Discussion

The spectra of the heterogeneous phantom specimens displayed first-order peak densities that were significantly greater than those of the homogeneous control samples [Figure 4(b)]. This trend was similar to the trend observed for breast tissue specimens [Figure 4(a)].[27] Phantoms with large fibers (250 μm diameter) showed the highest peak densities with values greater than 3x those of the controls. The peak densities for the 390-μm microspheres, however, did not follow this trend. This discrepancy, plus the high MAD values for the phantom specimens, are believed to be due to non-uniform mixing of the inclusions in the phantom gel plus entrainment of air bubbles.

The spectra of heterogeneous phantom specimens also displayed second-order spectral gradients that were significantly lower than homogeneous control samples [Figure 5(b)]. Again, the spectral gradient trend of the homogeneous (control) vs. heterogeneous (with inclusions) phantom samples was similar to the trend for breast tissue specimens [Figure 5(a)].[27] Although homogeneous breast pathologies (adenomas and fat necrosis) and phantom specimens can be differentiated from the more heterogeneous microstructures, differentiation between the individual heterogeneous classifications is more difficult, particularly for the phantom specimens. Again it is believed that this is due to non-uniform mixing and air-bubble entrainment.

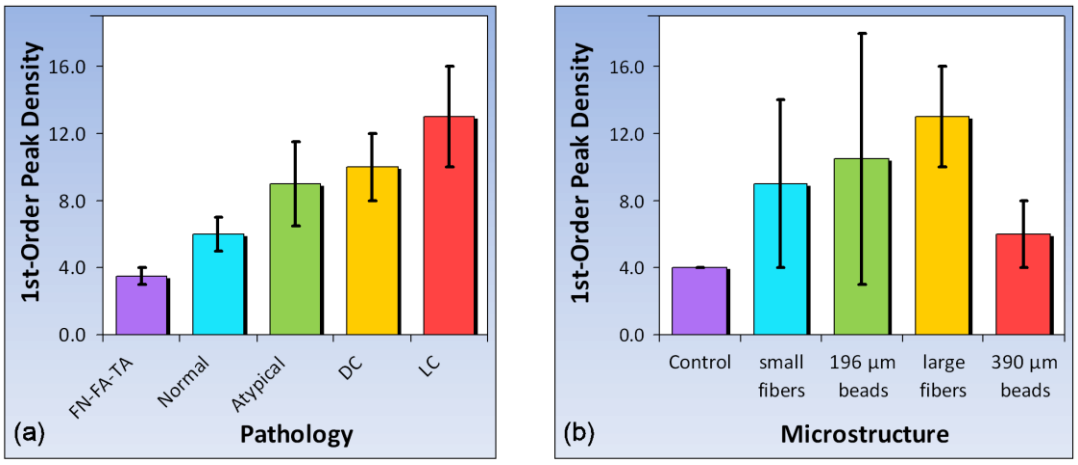

Figure 4. First-order peak densities in the 20-80 MHz band for margins and breast tissue specimens (a), and for phantom specimens (b). FN-FA-TA: fat necrosis, fibroadenoma, and tubular adenoma; Normal: normal breast tissue; Atypical: atypical ductal hyperplasia, fibrocystic changes, papilloma, and benign breast with calcifications; DC: ductal carcinomas (DCIS and IDC); LC: lobular carcinomas (LCIS and ILC).

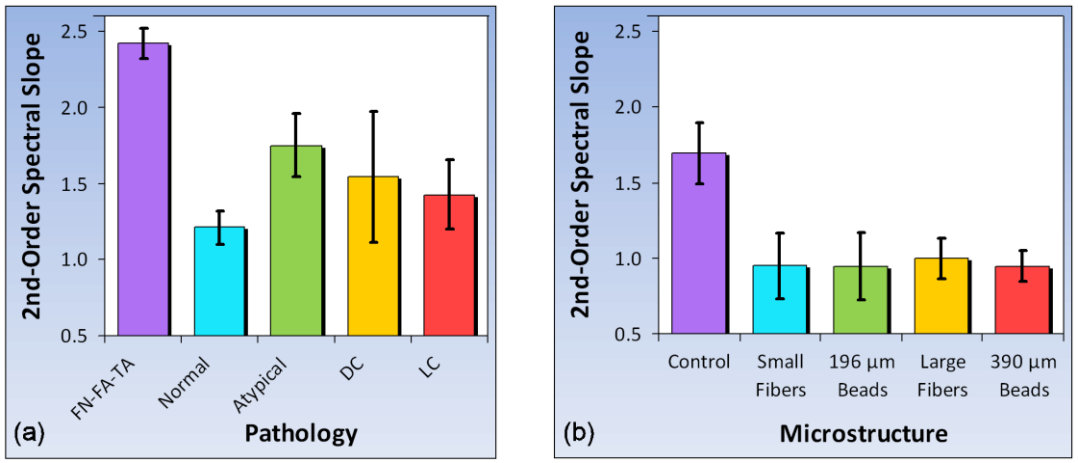

Figure 5. Second-order spectral gradients in the 20-80 MHz band for margins and breast tissue specimens (a), and for phantom specimens (b).

The results from Figures 4 and 5 indicate that the first-order peak density and second-order spectral gradient in HF ultrasonic spectra are linked to microstructural heterogeneity. In the phantom studies, the presence of inclusions increased the peak density and decreased the spectral gradient. These inclusions mimic the histopathology of the most common breast cancers, including those that fill the mammary ducts and lobules with malignant cells as in DCIS and LCIS, respectively, and those that form microtumors as in ILC and invasive ductal carcinoma (IDC). The breast tissue specimens showed trends that indicated that peak density increases [Figure 4(a)] and spectral gradient decreases [Figure 5(a)] with the level of tissue heterogeneity. These trends were observed to some extent for the phantom peak densities [Figure 4(b)] but mostly not observed for the phantom spectral gradients [Figure 5(b)]. The large median absolute deviations in the phantom peak densities and the lack of a trend for most of the phantom spectral gradients are probably due to the specimen mixing problems.

Since the peak density and spectral gradient are sensitive to the microstructure (pathology) of the tissue, the HF ultrasonic method can be regarded as a microanalytical approach as opposed to a strictly imaging approach. However, it would be relatively straightforward to expand these data acquisition and signal processing methods into an imaging modality. Microanalytical ultrasound would therefore be complementary to ultrasonic imaging, similar to the relationship between electron probe microanalysis and scanning electron microscopy. In this case, instead of

displaying ultrasonic density, the sonogram would display a dot map with each pixel conveying information about the pathology of that position in the imaged tissue. The information could most easily be conveyed using color to represent different pathology types (normal, fibroadenomas, ductal carcinomas, etc.).

4. Conclusions

Increased heterogeneity in simulated phantom and *in silico* tissues produced higher first-order peak densities and lower second-order spectral slopes, results consistent with data from resected margins. The results provide a physical mechanism for the use of these parameters in the imaging of breast tissues with atypical and malignant pathologies.

5. Acknowledgments

We gratefully thank Leigh Neumayer, Rachel Factor, Bryan Welm, Alana Welm, and our other colleagues in the Breast Disease-Oriented Team (BDOT) at the Huntsman Cancer Institute for their continuing support, assistance, and advice. We also thank Brent Bargeron and Sam Rushforth at Utah Valley University for their support of this research. This project was funded by a Grant for Engaged Learning (GEL) from Utah Valley University.

6. References

1. M. S. Anscher, P. Jones, L. R. Prosnitz, W. Blackstock, M. Hebert, R. Reddick, A. Tucker, R. Dodge, G. Leight Jr., J. R. Iglehart, and J. Rosenman, "Local failure and margin status in early-stage breast carcinoma treated with conservation surgery and radiation therapy," Annals of Surgery **218**, 22-28 (1993).
2. M. M. Moore, G. Borossa, J. Z. Imbrie, R. E. Fechner, J. A. Harvey, C. L. Slingluff Jr., R. B. Adams, and J. B. Hanks, "Association of infiltrating lobular carcinoma with positive surgical margins after breast-conservation therapy," Annals of Surgery **231**, 877-882 (2000).
3. M. M. Moore, L. A. Whitney, L. Cerilli, J. Z. Imbrie, M. Bunch, V. B. Simpson, and J. B. Hanks, "Intraoperative ultrasound is associated with clear lumpectomy margins for palpable infiltrating ductal breast cancer," Annals of Surgery, **233**, 761-768 (2001).
4. D. H. Roukos, A. M. Kappas, and N. J. Agnantis, "Perspectives and risks of breast-conservation therapy for breast cancer," Ann. Surg. Oncol. **10**, 718-721 (2003).
5. N. Cabioglu, K. K. Hunt, A. A. Sahin, H. M. Kuerer, G. V. Babiera, S. E. Singletary, G. J. Whitman, M. I. Ross, F. C. Ames, B. W. Feig, T. A. Buchholz, and F. Meric-Bernstam, "Role for intraoperative margin assessment in patients undergoing breast-conserving surgery," Ann. Surg. Oncol. **14**, 1458-1471 (2007).
6. A. W. Dick, M. S. Sorbero, G. M. Ahrendt, J. A. Hayman, H. T. Gold, L. Schiffhauer, A. Stark, and J. J. Griggs, "Comparative effectiveness of ductal carcinoma in situ management and the roles of margins and surgeons," J. Natl. Cancer Inst. **103**, 92-104 (2011).
7. R. A. Sakr, B. Poulet, G. J. Kaufman, C. Nos, and K. B. Clough, "Clear margins for invasive lobular carcinoma: a surgical challenge," Eur. J. Surg. Oncol. **37**, 350-356 (2011).
8. V. S. Klimberg, K. C. Westbrook, and S. Korourian, "Use of touch preps for diagnosis and evaluations of surgical margins in breast cancer," Ann. Surg. Oncol. **5**, 220-226 (1998).
9. J. C. D. Cendán, D. Coco, and E. M. Copeland, "Accuracy of intraoperative frozen-section analysis of breast cancer lumpectomy-bed margins," J. Am. Coll. Surg. **201**, 194-198 (2005).
10. T. P. Olson, J. Harter, A. Munoz, D. M. Mahvi, and T. Breslin, "Frozen section analysis for intraoperative margin assessment during breast-conserving surgery results in low rates of re-excision and local recurrence," Ann. Surg. Oncol. **14**, 2953-2960 (2007).
11. E. K. Valdes, S. K. Boolbol, J. M. Cohen, and S. M. Feldman, "Intra-operative touch preparation cytology; does it have a role in re-excision lumpectomy?," Ann. Surg. Oncol. **14**, 1045-1050 (2007).

12. S. Kennedy, J. Geradts, T. Bydlon, J. Q. Brown, J. Gallagher, M. Junker, W. Barry, N. Ramanujam, and L. Wilke, "Optical breast cancer margin assessment: an observational study of the effects of tissue heterogeneity on optical contrast," Breast Cancer Research **12**, R91 (2010).
13. A. Shimauchi, T. Yamada, A. Sato, K. Takase, S. Usami, T. Ishida, T. Moriya, and S. Takahashi, "Comparison of MDCT and MRI for evaluating the intraductal component of breast cancer," Amer. J. Roentgenology **187**, 322-329 (2006).
14. L. Bathla, A. Harris, M. Davey, P. Sharma, and E. Silva E, "High resolution intra-operative two-dimensional specimen mammography and its impact on second operation for re-excision of positive margins at final pathology after breast conservation surgery," Am. J. Surg. **202**, 387-394 (2011).
15. A. S. Haka, Z. Volynskaya, J. A. Gardecki, J. Nazemi, J. Lyons, D. Hicks, M. Fitzmaurice, R. R. Dasari, J. P. Crowe, and M. S. Feld, "*In vivo* margin assessment during partial mastectomy breast surgery using Raman spectroscopy," Cancer Res. **66**, 3317-3322 (2006).
16. A. S. Haka, Z. Volynskaya, J. A. Gardecki, J. Nazemi, R. Shenk, N. Wang, R. R. Dasari, M. Fitzmaurice, and M. S. Feld, "Diagnosing breast cancer using Raman spectroscopy: prospective analysis," J. Biomed. Opt. **14**, 054023 (2009).
17. F. Nguyen, A. M. Zysk, E. J. Chaney, J. G. Kotynek, U. J. Oliphant, F. J. Bellafiore, K. M. Rowland, P. A. Johnson, and S. A. Boppart, "Intraoperative evaluation of breast tumor margins with optical coherence tomography," Cancer Res. **69**, 8790-8796 (2009).
18. M. D. Keller, S. K. Majumder, M. C. Kelley, I. M. Meszoely, F. I. Boulos, G. M. Olivares, and A. Mahadevan-Jansen, "Autofluorescence and diffuse reflectance spectroscopy and spectral imaging for breast surgical margin analysis," Lasers Surg. Med. **42**, 15-23 (2010).
19. A. J. Fitzgerald, V. P. Wallace, M. Jimenez-Linan, L. Bobrow, R. J. Pye, A. D. Purushotham, and D. D. Arnone, "Terahertz pulsed imaging of human breast tumors," Radiology **239**, 533-540 (2006).
20. I. Pappo, R. Spector, A. Schindel, S. Morgenstern, J. Sandbank, L. T. Leider, S. Schneebaum, S. Lelcuk, and T. Karni, "Diagnostic performance of a novel device for real-time margin assessment in lumpectomy specimens," J. Surg. Res. **160**, 277-281 (2010).
21. M. Thill, K. Röder, K. Diedrich, and C. Dittmer, "Intraoperative assessment of surgical margins during breast conserving surgery of ductal carcinoma in situ by use of radiofrequency spectroscopy," Breast **20**, 579-580 (2011).
22. J. W. Jeong, D. C. Shin, S. H. Do, C. Blanco, N. E. Klipfel, D. R. Holmes, L. J. Hovanessian-Larsen, and V. Z. Marmarelis, "Differentiation of cancerous lesions in excised human breast specimens using multiband attenuation profiles from ultrasonic transmission tomography," J. Ultrasound Med. **27**, 435-451 (2008).
23. O. Olsha, S. Shemesh, M. Carmon, O. Sibirsky, R. A. Dalo, L. Rivkin, and I. Ashkenazi, "Resection margins in ultrasound-guided breast-conserving surgery," Ann. Surg. Oncol. **18**, 447-452 (2011).
24. K. M. Davis, C. H. Hsu, M. E. Bouton, K. L. Wilhelmson, and I. K. Komenaka, "Intraoperative ultrasound can decrease the re-excision lumpectomy rate in patients with palpable breast cancers," Am. Surg. **77**, 720-725 (2011).
25. N. M. Krekel, B. M. Zonderhuis, H. W. Schreurs, A. M. Cardozo, H. Rijna, H. van der Veen, S. Muller, P. Poortman, L. de Widt, W. K. de Roos, A. M. Bosch, A. H. Taets van Amerongen, E. Bergers, M. H. van der Linden, E. S. de Lange de Klerk, H. A. Winters, S. Meijer, and P. M. van den Tol, "Ultrasound-guided breast-sparing surgery to improve cosmetic outcomes and quality of life. A prospective multicentre randomised controlled clinical trial comparing ultrasound-guided surgery to traditional palpation-guided surgery (COBALT trial)," BMC Surg. **11**, 8 (2011).
26. C. Eichler, A. Hübbel, V. Zarghooni, A. Thomas, O. Gluz, M. Stoff-Khalili, and M. Warm, "Intraoperative ultrasound: improved resection rates in breast-conserving surgery," Anticancer Res. **32**, 1051-1056 (2012).
27. T. E. Doyle, R. E. Factor, C. L. Ellefson, K. M. Sorensen, B. J. Ambrose, J. B. Goodrich, V. P. Hart, S. C. Jensen, H. Patel, and L. A. Neumayer, "High-frequency ultrasound for intraoperative margin assessments in breast conservation surgery: a feasibility study," BMC Cancer **11**, 444 (2011).
28. R. O. Bude and R. S. Adler, "An easily made, low-cost, tissue-like ultrasound phantom material," J. Clin. Ultrasound **23**, 271-273 (1995).
29. T. E. Doyle, K. H. Warnick, and B. L. Carruth, "Histology-based simulations for the ultrasonic detection of microscopic cancer *in vivo*," J. Acoust. Soc. Am. **122**, EL210-EL216 (2007).
30. T. E. Doyle, A. T. Tew, K. H. Warnick, and B. L. Carruth, "Simulation of elastic wave scattering in cells and tissues at the microscopic cancer level," J. Acoust. Soc. Am. **125**, 1751-1767 (2009).

31. T. E. Doyle, H. Patel, J. B. Goodrich, S. Kwon, B. J. Ambrose, and L. H. Pearson, "Ultrasonic differentiation of normal versus malignant breast epithelial cells in monolayer cultures," J. Acoust. Soc. Am. **128**, EL229-EL235 (2010).